

ORIGINAL ARTICLE

Activation of *Evi1* inhibits cell cycle progression and differentiation of hematopoietic progenitor cells

OS Kustikova¹, A Schwarzer¹, M Stahlhut¹, MH Brugman^{1,2}, T Neumann¹, M Yang¹, Z Li¹, A Schambach¹, N Heinz¹, S Gerdes³, I Roeder³, TC Ha¹, D Steinemann⁴, B Schlegelberger⁴ and C Baum¹

The transcription factor *Evi1* has an outstanding role in the formation and transformation of hematopoietic cells. Its activation by chromosomal rearrangement induces a myelodysplastic syndrome with progression to acute myeloid leukemia of poor prognosis. Similarly, retroviral insertion-mediated upregulation confers a competitive advantage to transplanted hematopoietic cells, triggering clonal dominance or even leukemia. To study the molecular and functional response of primary murine hematopoietic progenitor cells to the activation of *Evi1*, we established an inducible lentiviral expression system. EVI1 had a biphasic effect with initial growth inhibition and retarded myeloid differentiation linked to enhanced survival of myeloblasts in long-term cultures. Gene expression microarray analysis revealed that within 24 h EVI1 upregulated 'stemness' genes characteristic for long-term hematopoietic stem cells (*Aldh1a1*, *Abca1*, *Cdkn1b*, *Cdkn1c*, *Epcam*, among others) but downregulated genes involved in DNA replication (*Cyclins* and their kinases, among others) and DNA repair (including *Brca1*, *Brca2*, *Rad51*). Cell cycle analysis demonstrated EVI1's anti-proliferative effect to be strictly dose-dependent with accumulation of cells in G₀/G₁, but preservation of a small fraction of long-term proliferating cells. Although confined to cultured cells, our study contributes to new hypotheses addressing the mechanisms and molecular targets involved in preleukemic clonal dominance or leukemic transformation by *Evi1*.

Leukemia (2013) 27, 1127–1138; doi:10.1038/leu.2012.355

Keywords: *Mecom*; gene therapy; MDS; transformation; transcription factor; quiescence

INTRODUCTION

The zinc finger transcription factor EVI1, encoded by the complex *Mecom* locus, is a master regulator of hematopoiesis. Its prominent oncogenic function was discovered using replicating retroviruses as insertional mutagens.¹ Insertional mutagenesis by replication-deficient retroviral vectors confirmed that activation of *Evi1* is a driver mutation establishing premalignant clonal expansion.^{2–5} Likewise, in human hematopoiesis, chromosomal rearrangements of *MECOM* on chromosome 3q26, or insertions of gene vectors containing strong enhancers, may activate *EVI1* and initiate a myelodysplastic syndrome (MDS), a slowly developing clonal disorder potentially progressing to acute myeloid leukemia (AML) of poor prognosis.^{6,7}

Evi1 deletion showed its essential and dose-dependent role in the maintenance of hematopoietic stem cells (HSC) and the propagation of leukemic cells.⁸ Next to EVI1, *Mecom* encodes an even larger MDS1-EVI1 fusion protein with an N-terminal PR-domain. The MDS1-EVI1 (or ME) protein may possess additional chromatin modifying activity, and was found to be essential for the quiescent long-term repopulating HSC (LT-HSC).⁹ A knock-in model showed that *Evi1* expression is also largely confined to quiescent LT-HSC,¹⁰ triggering the question whether *Evi1* induction is cause or consequence of HSC quiescence.

The role of the *Evi1* gene in the pathogenesis of leukemia was mostly investigated using mouse models and cell lines. Mice transplanted with bone marrow cells that expressed retrovirally transduced *Evi1* developed a MDS, indicating that *Evi1* induction

creates a preleukemic state and that additional genetic events are required for AML development. Indeed, clear evidence for leukemogenic cooperation of *Evi1* with other genes (among others, *Nras*) was obtained.^{11–14}

The first study of the immediate response to *EVI1* overexpression *in vitro* used a human myeloid leukemia cell line using a tetracycline-inducible vector system. This study revealed a dominant, dose-dependent negative effect of *EVI1* overexpression, causing an almost complete suppression of cells in the S phase and accumulation in G₀/G₁. However, it remained unclear how this anti-proliferative response was related to the transcriptome, whether it was also relevant for primary cells, and how it can be linked to the transforming potential of EVI1.¹⁵ More recently, using retroviral vectors that constitutively express *Evi1* in cultured murine hematopoietic cells, microarray studies revealed a mild but significant downregulation of the *Pten* tumor suppressor by the EVI1 protein, with further studies suggesting a link to long-term malignant progression.¹⁶

In the present study, we designed a robust, inducible expression system to examine the early functional and molecular response of primary murine hematopoietic progenitor cells to the induction of murine *Evi1*. We focused on the response of hematopoietic progenitor cells to understand how this transcription factor regulates proliferation and differentiation in the population that represents the vast majority of the cells transplanted in gene therapy, and the abundant population of a clone in the case of leukemogenic transformation. Furthermore, we examined the

¹Institute of Experimental Hematology, Hannover Medical School, Hannover, Germany; ²Department of Immunohematology and Blood transfusion, Leiden University Medical Center, Leiden, The Netherlands; ³Institute for Medical Informatics and Biometry, Medical Faculty Carl Gustav Carus, Dresden University of Technology, Dresden, Germany and ⁴Institute of Cell and Molecular Pathology, Hannover Medical School, Hannover, Germany. Correspondence: Dr C Baum, Institute of Experimental Hematology, OE6960, Hannover Medical School, Carl-Neuberg-Straße 1, 30625 Hannover, Germany.
E-mail: baum.christopher@mh-hannover.de

Received 3 September 2012; revised 21 November 2012; accepted 28 November 2012; accepted article preview online 5 December 2012; advance online publication, 8 January 2013

effects in cultured cells as studies performed in the context of gene therapy demonstrated that cytokine-rich cultures select for clones with insertional upregulation of *Evi1*.^{11,17–19} We demonstrate that *Evi1* has a biphasic effect on the proliferation of primary murine hematopoietic progenitor cells. The early growth suppression was characterized by accumulation of cells in G₀/G₁, upregulation of LT-HSC-specific genes, and downregulation of genes involved in DNA replication. In the presence of differentiation-inducing cytokines, the initial growth inhibition was followed by sustained but low-level long-term proliferation, impaired differentiation and enhanced survival of *Evi1*-expressing myeloblasts.

MATERIALS AND METHODS

Mice

C57BL/6J were purchased from Janvier (Le Genest-Saint-Isle, France), and kept in micro-isolators in the pathogen-free animal facility of Hannover Medical School. Rosa26rtTA-nls-Neo2 mice, kindly provided by Stefan Karlsson, Lund, Sweden, were bred with C57BL/6J (CD45.2) and genotyped as described.²⁰ Experiments were approved by the local ethical committee and performed according to their guidelines.

Vector construction

The coding complementary DNA (cDNA) of the murine *Evi1* gene (GenBank: M21829.1),¹ was equipped with a Kozak sequence, codon-optimized (Genscript Corporation, Piscataway, NJ, USA) removing cryptic splice and polyA sites to improve translation and mRNA half-life, and cloned via *AgeI* and *Sall* sites into a lentiviral self-inactivating (SIN) vector (pRRL.PPT.Tet.EGFP.pre) under the control of the tetP promoter.²¹ To track *Evi1* expression, we introduced enhanced green fluorescent protein (EGFP) via an internal ribosomal entry sequence derived from encephalomyocarditis virus in the *Sall* site downstream of *Evi1*. The pRRL.PPT.Tet.EGFP.pre vector was used as a control.

Cell lines, vector production and lentiviral transduction

Vectors were produced as previously described.²² In short, human embryonic kidney cells 293T were transfected with 10 µg of pRRL.PPT.Tet.Evi1RESEGFP.pre, 10 µg of pcDNA3.GP.4 × CTE (gag/pol), 5 µg of pRSV-Rev and 1.5–2 µg of pMD.G (VSVg) or pK73 (murine ecotropic envelope) using the calcium phosphate method. Supernatants were harvested and optionally concentrated using ultracentrifugation. Supernatants were titrated on SC1A3 cells, a subclone of murine fibroblast SC1 cells obtained after transduction with the vector ES1-2(M2RP) expressing the tetracyclin-dependent transactivator (rtTA).

Isolation, transduction and cultivation of primary cells

Bone marrow cells of Rosa26rtTA-nls-Neo2 mice were flushed out from femurs and tibias and lineage negative (Lin[−]) cells were magnetically sorted using lineage-specific antibodies (Lineage Cell Depletion Kit, Miltenyi Biotech, Bergisch Gladbach, Germany). Lin[−] cells were in StemSpan serum-free medium (Stem Cell Technologies, Vancouver, British Columbia, Canada) supplemented with 2% penicillin/streptomycin, 1% glutamine (both PAA) and one of the following cytokine cocktails (all cytokines from Peprotech, Hamburg, Germany): S3F11 = murine stem cell factor 50 ng/ml, murine interleukin 3 20 ng/ml, human FMS-like tyrosine kinase 3 ligand (hFlt-3) 50 ng/ml, and human interleukin 11 50 ng/ml;²³ or STIF = murine stem cell factor 50 ng/ml, murine thrombopoietin 20 ng/ml, murine insulin-like growth factor 2 20 ng/ml, human fibroblast growth factor 1 (hFGF-1) 10 ng/ml.²⁴ Following 24–48 h of pre-stimulation, Lin[−] cells were transduced overnight with lentiviral vectors (MOI of 2–20) on tissue culture plates coated with Retronectin (TaKaRa, Otsu, Japan). Doxycycline (DOX) was added 24 h after transduction. Transduction efficiency indicated by EGFP⁺ cells was measured 24 h after DOX induction. After 2 weeks of mass culture, limiting dilution was performed by seeding 50 cells per well in 96-well plates in S3F11 cytokines. Cell number and viability were determined using a CASY-TT instrument (Roche Diagnostics GmbH, Mannheim, Germany).

Flow cytometry and cell sorting

Expression of EGFP was detected by FACSCalibur flow cytometer (Becton Dickinson, Heidelberg, Germany). Cell cycle analysis was performed using the APC BrdU Flow kit (BD Pharmingen, San Jose, CA, USA) according to manufacturer's protocol. Data were acquired on a FACSCalibur flow cytometer. Raw data were processed using FlowJo software (Tree Star, Ashland, OR, USA). Dead cells were excluded by forward scatter and side scatter gating. Cells were sorted on FACSria or MoFlo instruments, supervised by the Cell Sorting Unit of Hannover Medical School.

Gene expression microarrays

Evi1/EGFP⁺ and control EGFP⁺ cells were sorted and total RNA was prepared using the RNeasy Micro Kit (Qiagen GmbH, Hilden, Germany). Material from three independent experiments (biological replicates) was generated. RNA quality was assessed using the Agilent 2100 Bioanalyzer (Agilent Technologies, Waldbronn, Germany). RNA was amplified by the Applause WT-Amp ST System (NuGEN Technologies, Bembel, The Netherlands), amplified cDNA was fragmented and biotin labeled using the Encore Biotin Module (NuGEN Technologies) according to manufacturer's protocol. Fragmented and labeled cDNA was hybridized to GeneChip Mouse Gene 1.0 ST Array (Affymetrix, High Wycombe, UK). For validation by real-time PCR and primer sequences, please refer to the Supplementary Information. Microarray data were submitted to the GEO database (<http://www.ncbi.nlm.nih.gov/geo>; accession number GSE39103).

Statistics and bioinformatics

Results were reported as the mean ± s.d. of individual data points obtained from varying numbers of experiments. Statistical significance was assessed by unpaired two-tailed Student's *t*-tests or Benjamini–Hochberg multiple testing as indicated below. Microarray data were analyzed using R and Bioconductor.²⁵ Data quality was assessed using the ArrayQualityMetrics package.²⁶ Arrays were background corrected, normalized and summarized using RMA.²⁷ LIMMA was used to detect differentially expressed probesets applying Benjamini–Hochberg multiple testing correction considering false discovery rate of <0.05 significant.²⁸ For testing enrichment of gene sets, the Broad Institute Gene Set Enrichment Analysis (GSEA) software package was employed.²⁹ The datasets were collapsed into single genes and rank-ordered by signal to noise ratio. 1000 Gene set permutations were used to estimate statistical significance. Analyzed gene sets were obtained from MSigDB v3.1 and GeneSigDB release 4.^{29,30}

See Supplementary Information for further details on microarrays analysis, immunoblots, real-time PCR, cell sorting, array-CGH and cytospin analysis.

RESULTS

An inducible system to over-express murine *Evi1* in primary hematopoietic progenitor cells

To address the early response of primary hematopoietic cells to *Evi1* overexpression we took advantage of the Rosa26rtTA-nls-Neo2 mouse, expressing the reverse tetracycline-inducible transactivator (rtTA) under the control of the ubiquitously active Rosa26 locus (Rosa26rtTA) for pharmacologically regulated induction of transgenes with rtTA-responsive promoters (tetP).²⁰

To avoid instability of the long *Evi1* message and enable robust expression, the coding sequence of the murine *Evi1* gene (GenBank: M21829.1)¹ was codon-optimized and cloned into a lentiviral SIN vector under control of the tetP promoter, linking EGFP via an internal ribosomal entry site (Figure 1a). The resulting protein sequence is identical to the original description of wild-type EVI1 (AAA40581.1, Supplementary Figures 1 and 2).¹ Compared to previously used gammaretroviral LTR-driven vectors, the lentiviral integration pattern and SIN configuration decreases but does not eliminate the risk of activating cellular proto-oncogenes as a result of insertional mutagenesis.^{31,32} The vector expressing EGFP only was used as a control.

To examine the early response of *Evi1* induction *in vitro*, Rosa26rtTA Lin[−] cells were prestimulated for 24 h in the S3F11 cytokine cocktail,²³ overnight transduced with the Evi1/EGFP or

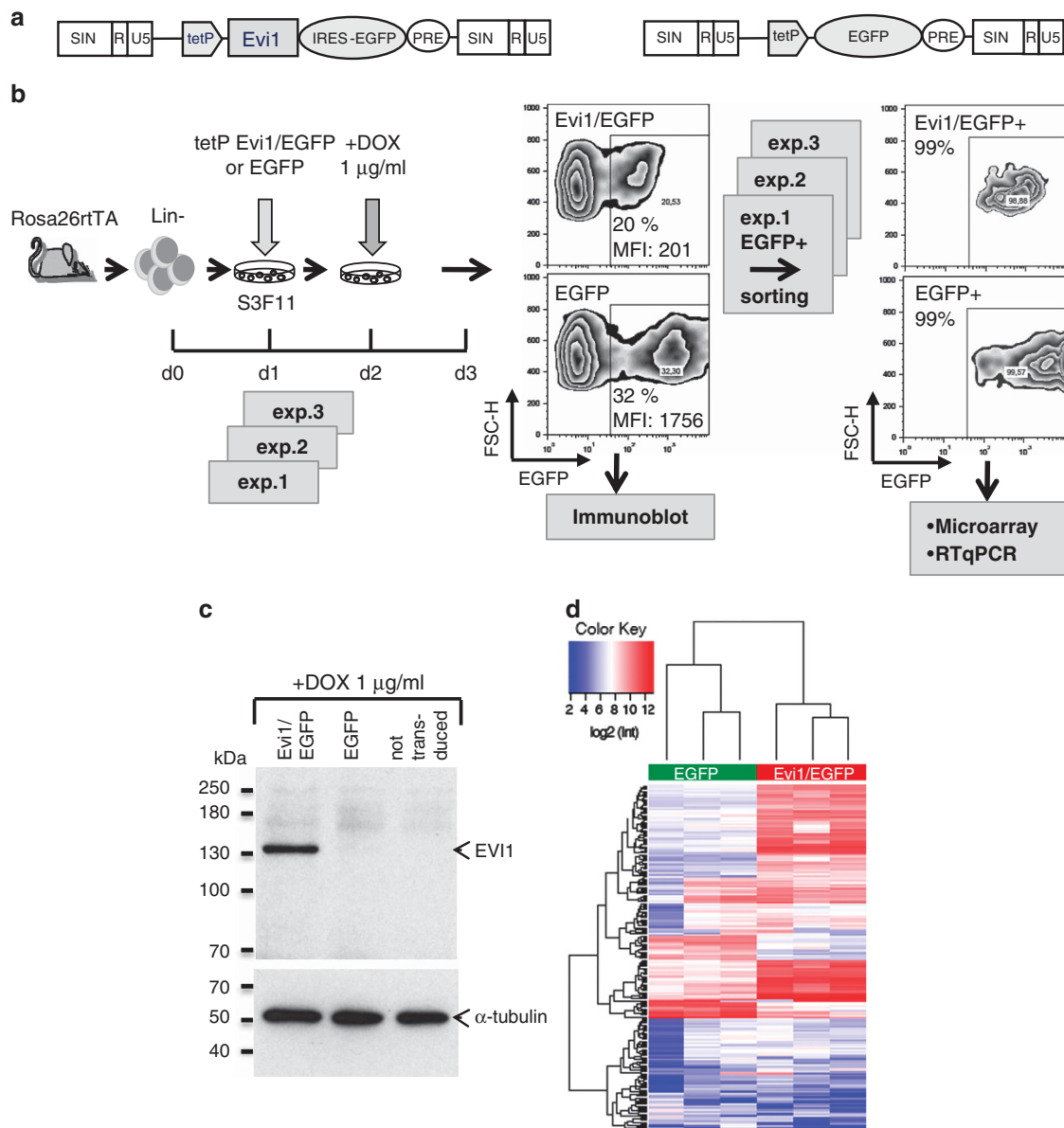


Figure 1. Establishing the inducible system to over-express codon-optimized murine *Evi1* in primary hematopoietic progenitor cells. **(a)** Vector design: the codon-optimized cDNA of the murine *Evi1* (*Evi1co*) was cloned into a lentiviral SIN vector under control of the tetP promoter. An internal ribosome entry site links *Evi1co* and EGFP. The vector expressing EGFP only was used as a control. **(b)** Schematic representation of experimental system. **(c)** Immunoblot demonstrates inducible EVI1 protein (in transduced primary murine hematopoietic progenitor cells, corresponds to day 3 in **(b)**). **(d)** Microarray analysis results observed for sorted *Evi1*/EGFP + and EGFP + cells after 24 h of *Evi1* expression in Lin – Rosa26rtTA cells. The heatmap shows the clear separation of the experimental groups obtained from three independent experiments, unsupervised hierarchical clustering of transcripts with a $\log_2\text{IQR} > 3.0$ (213 genes).

EGFP control vector, induced for 24 h with DOX (1 $\mu\text{g}/\text{ml}$) and sorted for *Evi1*/EGFP + or EGFP + cells (Figure 1b). Immunoblots showed the expected protein with an apparent molecular mass of ~ 145 kDa, induced by 1 $\mu\text{g}/\text{ml}$ DOX (Figure 1c). RTPCR with a primer set for codon-optimized *Evi1* (*Evi1co*) confirmed the presence of abundant transcripts in the *Evi1*/EGFP + sample (Supplementary Figure 3a).

Importantly, in the absence of DOX, Rosa26rtTA Lin – cells transduced with the *Evi1*/EGFP or the EGFP vector did not show any EGFP + cells (Supplementary Figure 3b).

Gene expression changes caused by *Evi1* upregulation

To identify the transcriptional changes caused within 24 h of *Evi1* induction in primary hematopoietic cells, we conducted the

experiment described in Figure 1b in three independent biological replicates. Genome wide expression profiling with RNA isolated from sorted *Evi1*/EGFP + or EGFP + cells provided highly reproducible effects mediated by EVI1, as shown by the clear separation of the *Evi1*/EGFP + and EGFP + groups by unsupervised hierarchical clustering (Figure 1d).

The lists of genes that exhibited ≥ 2 -fold difference and a BH-adjusted $P < 0.05$ for *Evi1*/EGFP + compared to EGFP + includes 587 upregulated transcripts and 619 downregulated transcripts (Supplementary Tables 1 and 2). Table 1 lists the top 40 genes up- or downregulated in *Evi1*/EGFP + compared to EGFP + cells.

To identify the pathways used to *Evi1* induction in primary hematopoietic cells, we used GSEA.²⁹ Among the 963 gene sets available from MSigDB_C5 (Gene Ontology Gene Sets), 106 were downregulated comparing *Evi1*/EGFP + and EGFP +

Table 1. Top 40 transcripts up- or downregulated in *Evi1*/EGFP+ compared with EGFP+ cells

Gene symbol	logFC	Fold change	P-value	Gene symbol	logFC	Fold change	P-value
<i>Ctsj</i>	5.658	50.479	3.34E-08	<i>Tcrg-V2</i>	-3.706	0.076	9.57E-08
<i>Rsad2</i>	4.981	31.596	1.39E-08	<i>Il1rl1</i>	-3.495	0.089	3.34E-07
<i>Ctsr</i>	4.786	27.582	1.24E-07	<i>Sh2d1b1</i>	-3.469	0.090	5.96E-05
<i>Ldhb</i>	4.658	25.255	5.17E-08	<i>Mmp8</i>	-3.447	0.092	0.0019102
<i>Spic</i>	4.585	24.000	4.26E-05	<i>Tph1</i>	-3.202	0.109	3.66E-05
<i>Chi3l1</i>	4.464	22.070	1.28E-05	<i>Cd33</i>	-3.067	0.119	3.55E-05
<i>Il18</i>	4.455	21.931	1.43E-05	<i>Nkg7</i>	-3.060	0.120	9.64E-07
<i>Slc6a20a</i>	4.402	21.141	3.81E-08	<i>Gpr65</i>	-2.959	0.129	0.0010638
<i>Pdzk1ip1</i>	4.237	18.854	5.54E-08	<i>Gpr141</i>	-2.898	0.134	0.0001156
<i>Hba-a2</i>	4.224	18.689	7.46E-08	<i>Fcgr3</i>	-2.876	0.136	2.03E-05
<i>Enkur</i>	4.167	17.967	4.23E-06	<i>Ngp</i>	-2.865	0.137	0.0011381
<i>Cfb</i>	4.126	17.459	1.35E-07	<i>Trem3</i>	-2.752	0.148	3.36E-06
<i>Fcer2a</i>	4.082	16.939	6.31E-07	<i>Lipg</i>	-2.733	0.150	2.02E-05
<i>Hba-a1</i>	3.957	15.531	1.27E-06	<i>Serpina1a</i>	-2.594	0.166	1.21E-05
<i>Ly6i</i>	3.950	15.453	3.25E-05	<i>Mpo</i>	-2.550	0.171	7.22E-05
<i>Them5</i>	3.796	13.893	2.81E-07	<i>Ctsj</i>	-2.549	0.171	3.01E-05
<i>Mt2</i>	3.778	13.7183	1.05E-05	<i>Eltd1</i>	-2.491	0.178	1.83E-05
<i>Ifit1</i>	3.691	12.914	0.0003734	<i>Cd69</i>	-2.476	0.180	7.11E-05
<i>Klf12</i>	3.690	12.905	1.21E-07	<i>Il7r</i>	-2.460	0.182	8.17E-05
<i>Akr1b8</i>	3.650	12.555	7.76E-07	<i>Ms4a2</i>	-2.457	0.182	1.59E-05
<i>Muc1</i>	3.635	12.422	4.26E-06	<i>Cd34</i>	-2.455	0.182	1.50E-05
<i>Naaa</i>	3.614	12.2430	1.31E-07	<i>Vcan</i>	-2.447	0.183	3.34E-05
<i>Gm4951</i>	3.569	11.865	0.0014281	<i>Srm</i>	-2.437	0.185	4.46E-05
<i>Ddx60</i>	3.539	11.623	0.0003763	<i>Slc7a5</i>	-2.398	0.190	2.49E-06
<i>Pgap1</i>	3.465	11.042	6.57E-08	<i>Mrgpra6</i>	-2.395	0.190	0.0011207
<i>Amigo2</i>	3.411	10.641	4.89E-07	<i>Ccr2</i>	-2.356	0.195	0.001438
<i>Slc16a4</i>	3.395	10.523	3.05E-05	<i>Ccr1</i>	-2.354	0.196	0.0018909
<i>Gbp2</i>	3.357	10.248	4.63E-06	<i>Ms4a3</i>	-2.321	0.200	4.19E-05
<i>ligp1</i>	3.347	10.179	0.0003917	<i>Olr1</i>	-2.321	0.200	0.0007363
<i>Ifit3</i>	3.336	10.102	0.0034252	<i>F2rl2</i>	-2.318	0.200	1.00E-05
<i>Sirpb1a</i>	3.309	9.914	0.0001118	<i>Hist1h2br</i>	-2.309	0.202	0.0030122
<i>Fn1</i>	3.250	9.512	6.17E-07	<i>Adora3</i>	-2.290	0.204	1.19E-05
<i>Sirpb1b</i>	3.230	9.383	0.0038013	<i>Hdc</i>	-2.289	0.204	0.0003319
<i>Epcam</i>	3.193	9.146	5.34E-06	<i>Elane</i>	-2.286	0.205	1.46E-05
<i>Gbp6</i>	3.158	8.924	0.0001342	<i>Mns1</i>	-2.255	0.209	0.0001336
<i>Ifit2</i>	3.156	8.915	0.0001926	<i>Lpl</i>	-2.249	0.210	0.0012255
<i>Myct1</i>	3.144	8.840	1.58E-05	<i>Cdh17</i>	-2.240	0.212	0.0002787
<i>Nqo1</i>	3.127	8.734	1.52E-06	<i>Atp8b4</i>	-2.230	0.213	2.88E-05
<i>Ube2l6</i>	3.125	8.725	1.44E-05	<i>Gpr97</i>	-2.212	0.216	1.14E-06
<i>Gm4841</i>	3.098	8.564	9.68E-05	<i>Il1r2</i>	-2.181	0.220	0.0019057

Abbreviation: FC, fold change. Only genes that exhibited ≥ 2 -fold difference in their expression between *Evi1*/EGFP+ and EGFP+ are presented. Only known, unique genes are listed; upregulated genes are in white field; downregulated genes are in gray field.

($P < 0.01$). Strikingly, the most gene sets downregulated in *Evi1*/EGFP+ cells were related to cell cycle progression (Table 2), even though cells were cultured in a cytokine-rich cocktail (Figure 2a).

Next, we explored the GeneSigDB database which focuses on cancer and stem cells gene signatures.³⁰ GSEA revealed that 315 from 2598 gene sets were upregulated in *Evi1*/EGFP+ cells at $P < 0.01$ compared with EGFP+. Interestingly, the second top score gene set enriched in *Evi1*/EGFP+ cells was overrepresented in murine LT-HSC (Table 3, Figure 2b).^{33–37} Supplementary Table 3 demonstrates an overlap of genes significantly ($P < 0.05$) upregulated in *Evi1*/EGFP+ cells and murine LT-HSC.³³ Among these genes are *Aldh1a1*, *Cdkn1c*, *Hoxa5*, *Hoxb5*, *Pbx1* and *Slamf1*. This overlap together with other markers (*Abca1*, *Cdkn1b*, *Epcam*, *Ly6a* (*Sca1*), Supplementary Table 1) revealed that the cell cycle suppression signature induced by EVI1 in primary hematopoietic progenitor cells is linked to the induction of LT-HSC associated gene sets (Figures 2c and d).

Another striking feature of the GSEA was the upregulation by *Evi1* of a large number of interferon pathway genes (Supplementary Tables 4 and 5). Interestingly, these do not contain the ligands (interferon α , β or γ , but rather downstream effectors, such as *Stat1*, *Stat2*, *Ly6i*, *Ly6a*, *Ifit1*, *Ifit3*, *Irf1*, *Irf7*, *Irf9*, etc.

(Supplementary Table 5). This suggests a broad effect of EVI1 on the regulation of cytokine signaling rather than an innate immune response caused in our experimental system. Note that the control populations went through the same lentiviral transduction and transgene induction protocol.

Additionally, we used another experimental design to study the early response of murine primary progenitor hematopoietic cells to *Evi1* overexpression, sorting *Evi1*/EGFP+ and *Evi1*/EGFP- cells after 24 h of DOX (microarray analysis in three technological replicas, Supplementary Figures 3c and d). The two microarray sets obtained from these different experimental systems demonstrated a very similar EVI1 signature (Figure 1b; Supplementary Figures 3c–f), characterized by downregulation of genes involved in cell cycle progression, upregulation of genes specific for LT-HSC and upregulation of interferon signaling genes. The interferon signature was not observed in the *Evi1*/EGFP- cells co-cultured with the *Evi1*/EGFP+ cells, consistent with the lack of induction of the Interferons by EVI1 and further arguing against an unspecific 'inflammatory' response. The experiment shown in Supplementary Figures 3c and d also revealed a significant downregulation of *Pten* (FC = 0.65; $P < 0.01$), as reported earlier.¹⁶

Table 2. Gene sets enriched in EGFP+ and downregulated in *Evi1*/EGFP+ cells (MSigDb_C5)

Gene set: <i>MsigDb_C5</i>	Source	Description	Genes upregulated in EGFP+ (leading-edge subset, 1 up to 25)	ES	NES	NOM P	FDR q
DNA_REPLICATION	Genes annotated by the GO term GO:0006260	The process whereby new strands of DNA are synthesized. The template for replication can either be an existing DNA molecule or RNA	<i>POLE, EXO1, ORC1L, RAD51, POLE2, POLD2, DKC1, CDC6, MCM3, MCM7, DUT, TIPIN, MCM2, ORC2L, MCM5, PRIM1, RPA2, POLD4, NASP, POLA1, NOL8, MLH1, DBF4, PRIM2, PMS1</i>	0.73	2.49	<0.001	<0.001
NUCLEOLUS	Genes annotated by the GO term GO:0005730	Present in the nucleus of eukaryotic cells; rich in RNA and protein; function: the transcription of the nucleolar DNA into 45S ribosomal-precursor RNA, the processing of this RNA into 5.8S, 18S, 28S	<i>RPP40, DKC1, UTP20, GNL3, LYAR, NSUN2, NOLC1, MYBBP1A, PARP1, MKI67IP, EXOSC1, NOC4L, GEMIN4, DDX21, POLA1, CIRH1A, NOL8, RPP38, RPP30, PNO1, TAF5, DDX56, MPHOSPH10, TOP2A, IKBKAP</i>	0.69	2.39	<0.001	<0.001
M_PHASE_OF_MITOTIC_CELL_CYCLE	Genes annotated by the GO term GO:0000087	Progression through M phase, the part of the mitotic cell cycle during which mitosis takes place	<i>KNTC1, TTK, KIF15, NDC80, CDC25C, NOLC1, PRMT5, AURKA, KIF2C, BUB1, CDCA5, CENPE, BUB1B, ATM, PLK1, NCAPH, TPX2, TGFB1, CCNA2, CIT, NEK2, RCC1, MAD2L1, ESPL1, ANLN</i>	0.71	2.36	<0.001	<0.001
CELL_CYCLE_PROCESS	Genes annotated by the GO term GO:0022402	A cellular process that is involved in the progression of biochemical and morphological phases and events that occur in a cell during successive cell replication or nuclear replication events	<i>POLE, RAD51L1, RAD51, CDC7, CHEK1, CDC6, BCAT1, KNTC1, BRCA2, RAD54L, TIPIN, CDK6, TTK, KIF15, FBXO5, TUBE1, NDC80, RAD1, CDC25C, NOLC1, PRMT5, AURKA, KIF2C, TUBG1, BUB1</i>	0.63	2.35	<0.001	<0.001
MITOTIC_CELL_CYCLE	Genes annotated by the GO term GO:0000278	Progression through the phases of the mitotic cell cycle, which comprises phases G1, S, G2 and M and includes replication of the genome and the segregation of chromosomes into daughter cells	<i>POLE, CDC7, CDC6, BCAT1, KNTC1, CDK6, TTK, KIF15, FBXO5, NDC80, CDC25C, NOLC1, PRMT5, AURKA, KIF2C, BUB1, CDCA5, CENPE, BUB1B, ATM, SKP2, PLK1, NCAPH, POLA1, TPX2</i>	0.64	2.32	<0.001	<0.001

Abbreviations: ES, enrichment score; FDR, false discovery rate; GO, gene ontology; NES, normalized enrichment score; NOM P, nominal P value. The top 5 scoring gene sets presented. MSigDb collection, C5: GO gene sets.

Early response to *Evi1* induction: inhibition of cell cycle progression

Statistical analyses confirmed overall stability of gene expression within the input groups and identified the biological effect caused by overexpression of *Evi1* as the main source of variation (Supplementary results, Supplementary Figure 4 and Supplementary Table 6). To validate the transcriptional response of *Cyclin* genes important for cell cycle progression, we used real-time PCR. Indeed, all *Cyclins* investigated were significantly downregulated in *Evi1*/EGFP+ versus control EGFP+ cells (Figure 2e). The strongest downregulation was observed for *Ccne1*, *Ccne2*, *Ccna2*, *Ccnd1* ($P < 0.0001$), and *Ccnd2* ($P = 0.0025$). Benjamini–Hochberg multiple testing correction confirmed the significance (*Ccne1* adj. $P = 3.54000E - 09$; *Ccne2* adj. $P = 1.92300E - 12$; *Ccna2* adj. $P = 7.37375E - 07$; *Ccnd1* adj. $P = 7.37375E - 07$; *Ccnd2* adj. $P = 6.95300E - 03$). Interestingly, *Ccnd3* was an exception with slight upregulation in the microarrays (1.231-fold, $P = 0.02$).

Evi1 induction also repressed the Cyclin-dependent kinases, whereas the opposite was true for the cell cycle inhibitory genes encoding p18, p27 and p57. The most prominent effects were seen for *Cdkn1c* (p57: 2.48-fold elevated, $P = 6.21E - 06$) and *Cdkn1b* (p27: 2.173-fold elevated, $P = 0.002$) (Supplementary Table 1, Figure 3a). *Evi1* upregulation for 24 h thus induced a pronounced arrest in G_0/G_1 (Figure 3b). This response was dose

dependent: cells expressing *Evi1*/EGFP at the highest level showed an almost complete loss of the S phase (Figures 3c–e). Importantly, *EV1* protein levels determined by immunoblot correlated well with the mean fluorescence intensity of EGFP and the concentration of DOX used (Figure 3c, Supplementary Figure 5a). EGFP alone had no effect on the cell cycle, irrespective of the dose (Figures 3d and f). The quiescence-inducing effect of *EV1* also occurred in cytokine conditions lacking IL3 (STIF cocktail)²⁴ (Supplementary Figure 5b).

The initial growth inhibition is followed by enhanced survival of *Evi1*-expressing myeloblasts

To determine how *Evi1* confers a selective advantage to cultured murine hematopoietic progenitor cells, *Evi1*/EGFP and control EGFP mass cultures were grown in liquid cultures in the presence of cytokines for 9–14 days followed by limiting dilution (three independent experiments, Figure 4a). In an effort to exclude insertional activation of proto-oncogenes due to the lentiviral vector integration,³¹ a low transduction rate of Rosa26rtTA Lin – cells (below 10% of EGFP+ cells) was used (experiments 1 and 2). Increasing the transduction rate up to 20% of EGFP+ cells (experiment 3) resulted in the selection of cultures with extended survival from both, *Evi1*/EGFP and control EGFP groups (data not shown).

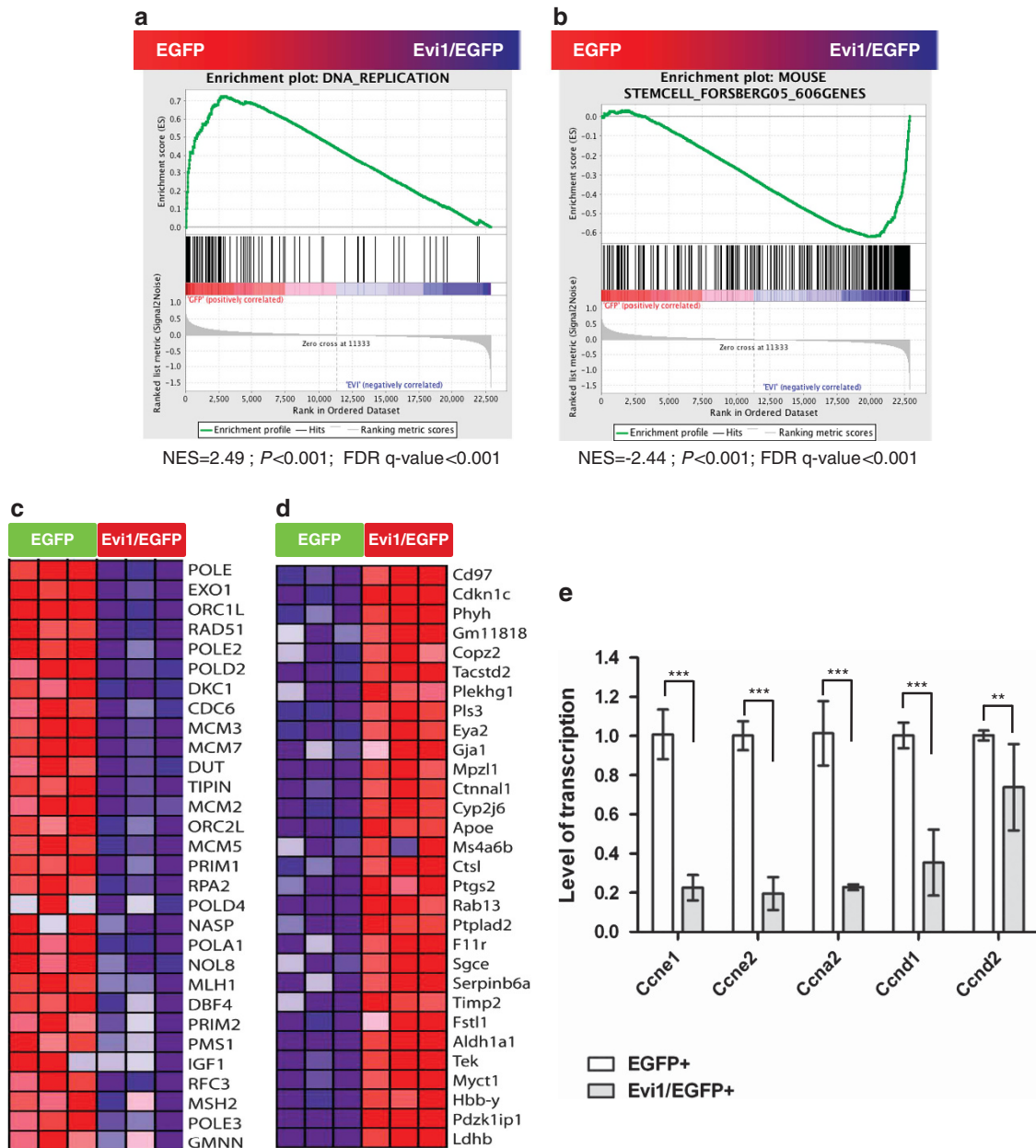


Figure 2. Gene expression changes caused by 24 h of *Evi1* upregulation in primary hematopoietic progenitor cells. **(a)** Selected gene set from GSEA containing genes upregulated in control EGFP and downregulated in Evi1/EGFP samples (DNA replication). **(b)** Selected gene set containing genes downregulated in control EGFP and upregulated in Evi1/EGFP samples (genes associated with transcriptome of long-term hematopoietic stem cells (LT-HSC) compared with multipotent progenitors.³³ NES, normalized enrichment score. FDR, false discovery rate. **(c)** The top 30 list of genes upregulated in control EGFP and downregulated in Evi1/EGFP samples, corresponding to **a**. **(d)** The top 30 list of genes downregulated in control EGFP and upregulated in Evi1/EGFP samples, corresponding to **b**. **(e)** Validation of microarray data and confirmation on transcriptional level of early growth inhibition effect of *Evi1* expression. Real-time PCR analysis of Cyclins in sorted Evi1/EGFP+ and EGFP+ cells, 24 h after *Evi1* induction with 1 μ g/ml DOX; material from three independent experiments in triplicates. Data are represented as mean \pm s.d., $n = 9$, *** $P < 0.0001$, ** $P = 0.0025$.

Strikingly, morphological examination (cytospin analysis, scoring at least 100 cells per condition) revealed a high percentage of myeloblasts and promyelocytes upon ectopic expression of *Evi1*. In contrast, control EGFP cultures predominantly demonstrated the phenotype of mast cells or mature monocytes (Figure 4a). Only three cultures obtained after limiting dilution (Evi1/EGFP9, Evi1/EGFP6 and EGFP5) continued growth for maximum 40 days after cryopreservation (Figure 4b). Thus, despite the initial growth suppression in the first 2 weeks

after *Evi1* induction, prolonged induction induced a survival advantage for myeloblasts, revealing a relative inhibition of myeloid differentiation. A full transformation to permanent growth was not observed in our experimental system.

To study how *Evi1* downregulation influences the fate after long-term cultivation, we washed the cells of the most robustly growing culture, Evi1/EGFP6, and withdrew DOX. Flow cytometry revealed downregulation of EGFP within 48 h (Figure 4c). Importantly, cell viability was reduced on day 5, extinguishing the

Table 3. Gene sets enriched in *Evi1*/EGFP + cells (GeneSigDb)

Gene set	Source	Description	Genes upregulated in <i>Evi1</i> /EGFP + (leading-edge subset, 1 up to 25)	ES	NES	NOM P	FDR q
HUMAN STEMCELL_49GENES	Jaitin et al. ³⁴	Transcripts upregulated in WISH cells treated with IFN-beta or functionally similar IFN-alpha2 mutant followed by anti-proliferative effect	<i>PSMB10, TNFSF10, SP110, PSME2, IFIH1, PSMB9, CASP7, CASP4, USP18, IRF9, CASP1, STAT2, IRF7, DDX58, MX2, TLR3, MX1, STAT1, IRF1, OAS2, ISG15, TSPAN8, IFIT1, IFIT3, RSAD2</i>	-0.86	-2.47	<0.001	<0.001
MOUSE STEMCELL_606GENES	Forsberg et al. ³³	Transcripts upregulated in LT-HSC compared with MPP	<i>Tacstd2, Plekhg1, Pls3, Eya2, Gja1, Mpzl1, Ctnnal1, Cyp2j6, Apoe, Ms4a6b, Ctsl, Ptgs2, Rab13, Ptplad2, F11r, Sgce, Serpinb6a, Timp2, Fstl1, Aldh1a1, Tek, Myct1, Hbb-y, Pdzk1ip1, Ldhh</i>	-0.62	-2.44	<0.001	<0.001
HUMAN IMMUNE_85GENES	Kulaeva et al. ³⁵	Transcripts downregulated at immortalization step but upregulated after demethylation following treatment of immortal LFS fibroblasts with 5AZA-dC (senescence-like state). A total of 39 transcripts (46%) are known to be regulated during interferon signaling	<i>TNFSF10, RRAD, IFI30, TDRD7, BST2, ISG20, CXCL2, OPTN, TNFAIP6, HTATIP2, CXCL3, TNFAIP2, ABCC3, IRF7, MX2, MX1, STAT1, CLU, OAS2, ISG15, UBE2L6, SLC16A4, IFI44, IFIT3, RSAD2</i>	-0.77	-2.42	<0.001	<0.001
HUMAN LUNG_DAUER05_50GENES REPRESSED	Dauer et al. ³⁶	Transcripts downregulated in A549 cells (lung cancer) expressing STAT3 off an adenovirus vector	<i>TNFSF10, SP110, TDRD7, IFIH1, USP18, OAS3, ST8SIA4, PDK4, IRF7, DDX58, PARP12, TLR3, HERC5, MX1, STAT1, OAS2, ISG15, IFI44, DDX60, IFIT1, IFIT3</i>	-0.83	-2.42	<0.001	<0.001
HUMAN BREAST_EINAV05_34GENES	Einav et al. ³⁷	Transcripts upregulated in childhood lymphoblastic leukemia and in breast and ovarian cancer, demonstrating a strong signature of an interferon-induced pathway	<i>SP100, ADAR, SP110, IFI30, TDRD7, BST2, PSME2, IRF9, RXRA, IRF7, MX1, STAT1, OAS2, ISG15, UBE2L6, IFI44, IFIT1, IFIT3</i>	-0.86	-2.37	<0.001	<0.001

Abbreviations: 5AZA-dC, 5-Aza-2 deoxycytidine; ES, enrichment score; FDR, false discovery rate; LFS, Li-Fraumeni syndrome; LT-HSC, long-term repopulating hematopoietic stem cell; MPP, multipotent progenitor; NES, normalized enrichment score; NOM P, nominal P value. The top 5 scoring gene sets presented.

culture until day 7 (Figure 4d), whereas the DOX-induced control contained healthy cells with proliferating blasts (Figure 4c). Although *Evi1* transcript levels at day 2 were still in the range of 50% on day 0 (Figure 4e), we found a marked differentiation shift: myeloblasts were lost (from 24 to 5%), while promyelocytes increased (from 24 to 46%; see insert for day 2 in Figure 4c). These data indicate that *Evi1* has a biphasic effect: the early growth inhibition is followed by a survival advantage of myeloblasts, associated with a relative block of differentiation, which depends upon the continued expression of *Evi1*.

Enhanced survival of *Evi1*-expressing myeloblasts

Having observed that *Evi1* inhibits or delays myeloid differentiation in long-term cultured cells (Figure 4c), we addressed whether the growth suppression observed in freshly induced cells also persisted over time. Interestingly, for all three independent experiments (Figure 4a), less than 1% of *Evi1*/EGFP + cells were observed by flow cytometry at the day of limiting dilution (data not shown), whereas in the EGFP control mass culture almost no loss of marked cells was detected within 14 days of DOX induction. The anti-proliferative effect of *Evi1* thus continued for at least 2 weeks in our experimental conditions.

In the resulting long-term cultures, insertional or other genotoxic or epigenetic events might have contributed to clonal selection: for example, for the *Evi1*/EGFPC6 culture, lentiviral integration analysis by LMPCR showed an insertion into the *Brca1* locus and for *Evi1*/EGFPE9 into *Angpt1* (data not shown). The integration into *Brca1* was intriguing as GSEA revealed that *Evi1* overexpression suppressed genes involved in DNA repair ($P < 0.001$), including *Brca1* (Supplementary Figures 6a and b). To identify potential secondary mutations caused by genetic instability, we performed array-based comparative genome hybridization of *Evi1*/EGFPC6 culture, for which we had sufficient genomic DNA to conduct this analysis. Besides some minor copy number variations, we observed a microdeletion of *Cullin3*, an E3 ubiquitin ligase associated with hematopoietic lineage priming and transformation (Supplementary Figures 6c and d).³⁸ We conclude that both, insertional mutagenesis and *Evi1*'s interference with genomic stability, complicate the study of delayed consequences of its ectopic overexpression.

We thus decided to analyze *Evi1*'s delayed effect on the cell cycle in newly established cultures: Rosa26rtTA Lin- cells transduced with tetP *Evi1*/EGFP or tetP EGFP vector were maintained as mass cultures in three biological replicas for 3 weeks in the presence of DOX (0.1 or 1.0 µg/ml) and S3F11

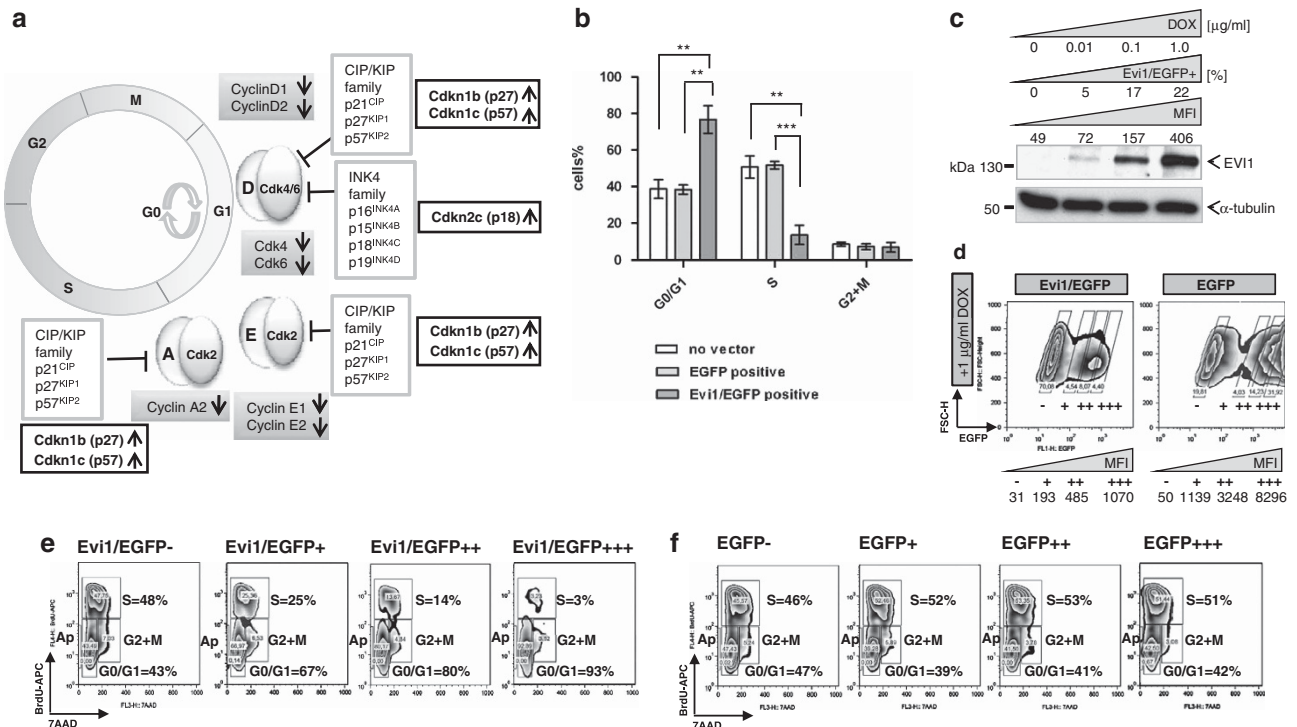


Figure 3. Cell cycle analysis confirmed early anti-proliferative effects of *Evi1* in cultured primary hematopoietic progenitor cells. **(a)** Microarray data summary: downregulation of Cyclins and upregulation of Cdk inhibitors; modified from Tesio and Trumpp.⁵⁶ **(b–f)** Dose-dependent anti-proliferative effects of *Evi1* (S3F11 cytokine conditions). **(b)** BrdU/7AAD cell cycle analysis histogram: EGFP has no effect on the cell cycle; a reduction of cells in S phase is only seen when inducing *Evi1* in conjunction with EGFP (for cell cycle analysis Evi1/EGFP+ and EGFP+ cells were gated). Data are represented as mean \pm s.d., $n = 3$, *** $P = 0.0003$, ** $P < 0.002$. **(c)** Level of inducible EVI1 protein (immunoblot analysis, 24 h after DOX induction) related to EGFP expression. MFI, mean fluorescence intensity of EGFP. **(d–f)** Gating strategy and cell cycle analysis, plot presentation: Gating EGFP–, EGFP+, EGFP++, and EGFP+++ populations for cell cycle analysis demonstrated dose-dependent anti-proliferative effects of *Evi1*.

cytokine conditions (Supplementary Figure 7a). Cell cycle analysis comparing Evi1/EGFP+ and EGFP+ expressing cells at day 1 and day 21 after DOX induction perfectly reproduced the early growth-inhibitory effect mediated by *Evi1* at day 1, even at a reduced level of induction using 0.1 μ g/ml of DOX (Figure 5a). However, after 3 weeks, all cultures including 'no vector' and control (EGFP) predominantly contained resting cells (>80% G₀/G₁ fraction, Figure 5b, (Supplementary Figures 7b–d).

Importantly, closer examination of the cells long-term (21 days) exposed to S3F11 cytokine conditions showed a small (<10%) but significantly increased S phase population in the presence of *Evi1* (Figure 5b). Comparable early and delayed effects of *Evi1* were obtained in similar experimental systems when transducing more primitive LSK (Lin^{neg/lo} Sca1^{high} Ckit^{high}) Rosa26rtTA cells with tetP Evi1/EGFP or tetP EGFP vectors and inducing gene expression at 1.0 μ g/ml DOX (Supplementary Figures 8a and b). Cytospin analysis of Evi1/EGFP+ and EGFP+ sorted cells at day 23 showed that the maintenance of proliferative activity was connected to the preservation of immature cells (myeloblasts, promyelocytes, myelocytes, metamyelocytes) (Figure 5c), which together formed ~50% of the *Evi1*-overexpressing population, whereas cells transduced with EGFP only had <10% immature cells left (Figure 5d, represented as mean \pm s.d., $n = 4$ (combined Rosa26rtTA Lin– and LSK data), *** $P = 0.0004$). Collectively, our data indicate that *Evi1* induction, while impeding cell cycle progression by a concerted repression of Cyclins and Cyclin-dependent kinases and activation of the respective inhibitors (*Cdkn* family), maintains a low but significant level of proliferative activity under conditions that lead to an irreversible differentiation of regular hematopoietic cells.

DISCUSSION

To investigate the response of hematopoietic progenitor cells to *Evi1* upregulation, we established an inducible lentiviral vector, allowing clear separation of induced and control populations. As our attempts to generate high-titer lentiviral vectors were unsuccessful when using vectors with a conventional cDNA, we codon-optimized the expression unit. The resulting vectors had sufficient titers and mediated a robust expression switch, allowing the assessment of dose-dependent effects from a low-vector copy number. Using this system, *Evi1* overexpression confers a selective advantage to primary hematopoietic progenitor cells that are cultured long-term in a myeloid cytokine cocktail. This observation perfectly recapitulates findings made with insertional upregulation of the endogenous allele.¹² In cells adapted to *Evi1* overexpression, its withdrawal induced a myeloid differentiation shift followed by rapid cell death, similar to observations made after transfection of a tetracyclin-inducible human (non codon-optimized) *EVI1* construct in U937 cells.¹⁵ Thus, basic functional properties of *Evi1* induction and adaptation were recapitulated in our approach.

Microarray studies of freshly transduced primary hematopoietic cells 24 h after *Evi1* induction revealed the regulation of important HSC markers (*Aldh1a1*, *Abca1*, *Cdkn1b*, *Cdkn1c*, *Epcam*, *Hoxa5*, *Hoxb5*, *Ly6a* (*Sca1*), *Pbx1* and *Slamf1*, among others). In line with and extending recent reports,^{8,10} the EVI1 protein can thus be viewed as a master regulator and not a consequence or simple marker of the HSC status.

The main focus of the present study is the negative impact of *Evi1* upregulation on cell proliferation hematopoietic progenitor

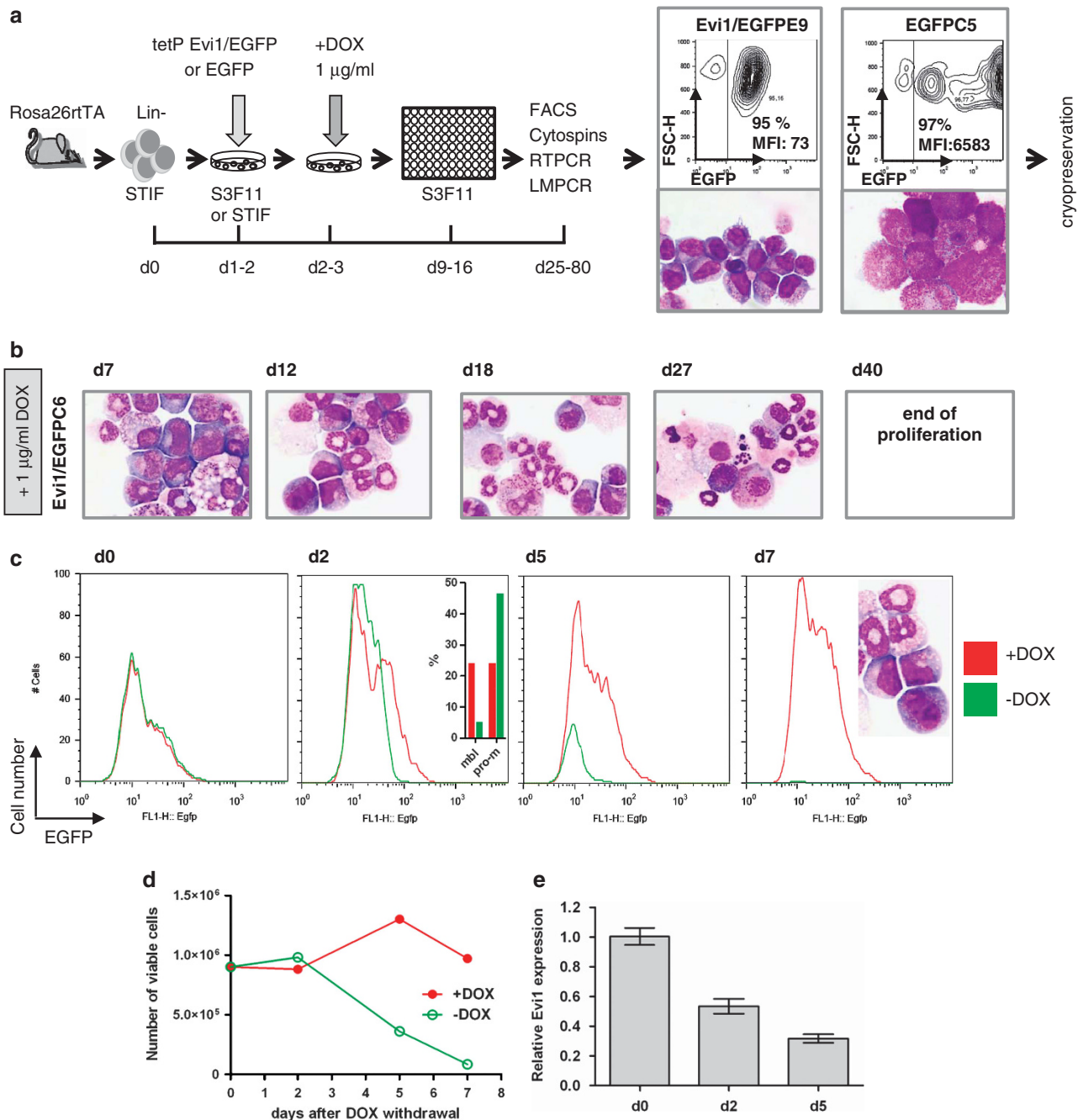


Figure 4. Initial growth inhibition followed by enhanced survival of *Evi1*-expressing cells. **(a)** Experimental design to study the delayed effect of *Evi1* in cultured primary murine hematopoietic progenitor cells. **(b)** *Evi1*/EGFP cells after cryopreservation survive in liquid culture for 40 days in the presence of S3F11 cytokines and 1 µg/ml DOX (cytospin analysis, May-Grünwald/Giemsa staining; magnification, $\times 1000$). **(c)** *Evi1*/EGFP cell survival depends on *Evi1*. 48 h (d2) after DOX withdrawal (– DOX, green) *Evi1*/EGFP cells had a reduced amount of myeloblasts (mbl) and increased promyelocytes (pro-m) compared with + DOX (red) (histogram insert). On day 7, no live cells were detected in the absence of DOX, whereas the DOX + cells continued to contain proliferating blasts (cytospin insert). **(d)** DOX dependence of *Evi1*/EGFP cells. Viable cell number measured by CASY at the indicated time points after DOX withdrawal. **(e)** Real-time PCR analysis of *Evi1* expression in *Evi1*/EGFP cells after DOX withdrawal (data are represented as mean \pm s.d., $n = 3$). d0, d2, d5 correspond to day 0, 2 and 5 without DOX.

cells, which may be paradoxical at first glance, as *Evi1* is a potent oncogene connected to high-risk AML^{6,7,16}. However, in a progressive clonal disease such as AML, adaptive genetic or epigenetic events, such as the unregulated activation of the RAS pathway^{13,39,40} may compensate initial anti-proliferative effects of *Evi1*. Such compensatory genes could be located on the human chromosome 7, explaining the selection for monosomy 7 in AML, although our analyses gave no clear evidence that *Evi1* suppresses

gene sets located on the human chromosome 7 (data not shown). Also relevant to the tumorigenic potential of *Evi1* upregulation is the question whether the cell cycle arrest observed in our study reflects a canonical senescence pattern. As the cell cycle break induced by *Evi1* was immediate, this pattern of 'oncogene-induced quiescence' is distinct from the well-known senescence observed after DNA damage or proliferation-inducing oncogenes such as RAS.^{41,42} While DNA repair genes were downregulated

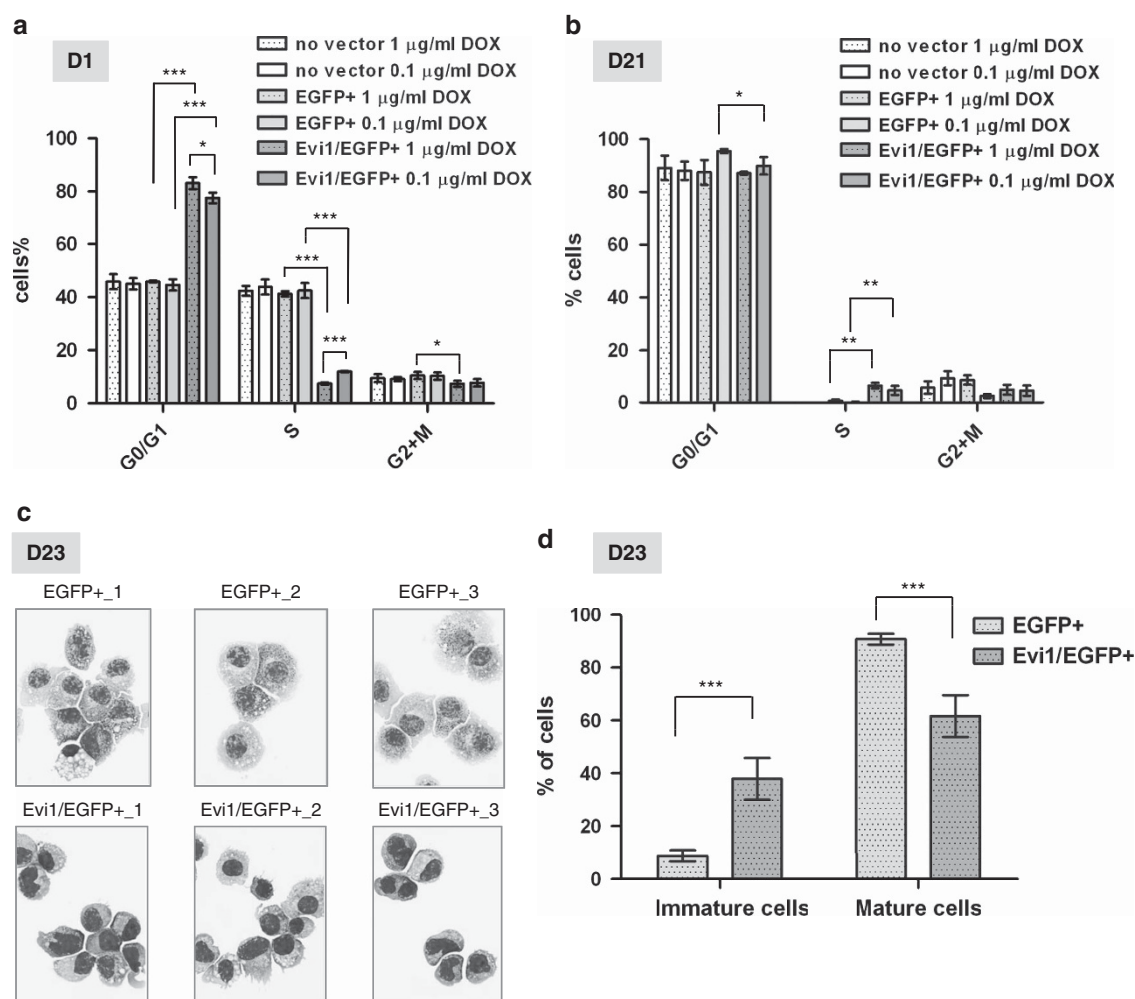


Figure 5. *Evi1*'s impact on cell cycle progression and differentiation over time. (a) Cell cycle histogram summary at day 1 after *Evi1* induction in Lin – Rosa26rtTA cells with 1 μ g/ml or 0.1 μ g/ml DOX: A higher DOX dose increased the % of cells in G₀/G₁ and lowered % in S phase for Evi1/EGFP + cells (S3F11 cytokine conditions). Data are represented as mean \pm s.d. $n = 3$, *** $P \leq 0.0002$, * $P < 0.05$. (b) Cell cycle analysis histogram at day 21: Evi1/EGFP + cells demonstrated increased proliferative activity in comparison with EGFP + or 'no vector' cells. Data are represented as mean \pm s.d., $n = 3$, ** $P \leq 0.001$, * $P < 0.05$. (c) Representative cytology (May-Grünwald/Giemsa staining; magnification, $\times 1000$) of sorted Evi1/EGFP + and EGFP + cells ($n = 3$) at day 23 after *Evi1* induction in LSK cells (1 μ g/ml DOX). (d) Histogram presentation of cytological analysis demonstrating a significantly increased amount of immature cells in Evi1/EGFP + samples (scoring at least 100 cells per condition). Immature cells: myeloblasts, promyelocytes, myelocytes, metamyelocytes. Mature cells: band neutrophils, segmented neutrophils, monocytes, macrophages, mast cells. Data are represented as mean \pm s.d., $n = 4$ (combined Rosa26rtTA Lin – and LSK data), *** $P = 0.0004$.

after *Evi1* induction, potentially contributing to the genetic instability associated with its overexpression,^{43,44} genotoxic stress was not found to trigger an immediate cell cycle arrest.⁴¹ In further support of this distinction is our finding of a downregulation of Trp53 (FC=0.58; $P < 0.0001$) as the immediate response to *Evi1* induction. While the upregulation of interferon-response genes (Table 3, Supplementary Table 4), has been identified in senescent cells,^{35,42} we found this signature to be conserved in fully transformed human AML associated with *EVI1* upregulation (Supplementary Figure 9).⁴⁵ Furthermore, we found the *Evi1* response to be associated with a block of differentiation and the preservation of a small fraction of proliferating cells. The rapid quiescence evoked by *Evi1* induction thus cannot be interpreted as the canonical pattern of either oncogene-induced or proliferative senescence. The velocity of the response to *Evi1* is rather reminiscent of the *Pten*-loss induced cellular senescence previously described for epithelial cells and fibroblasts,⁴⁶ not necessarily arguing that Evi1-mediated suppression of *Pten*,¹⁶ is the causal event in our system. Nevertheless, we would propose that oncogenic events inducing

immediate quiescence (such as *Pten* loss or *Evi1* upregulation) synergize with oncogenes that tend to induce proliferative senescence (RAS type) in the establishment of highly malignant, therapy-resistant cancers. The time to progression would thus only depend upon the acquisition of a crucial compensatory mutation. Our experimental data, further supported by mathematical modeling (data not shown), suggest a selection for 'just the right' dose of *Evi1* induction. This profound dose dependence may contribute to the emergence of defined clusters of common insertion sites after retroviral insertional mutagenesis,^{5,44,47} by counterselecting integration sites inducing a too high induction of *Evi1*. However, malignant cells with genetic or epigenetic induction of proliferative pathways may tolerate higher *Evi1* levels better than naïve primary cells.

Focusing on cell cycle-associated genes, we showed a concerted and dose-dependent downregulation of *Cyclin* genes and associated *Cdks* by *EVI1*, and an increase of the inhibitory *Cdkns*, predominantly *Cdkn1c* (p57). The latter is essential for maintaining the quiescence of HSC,⁴⁸ and is induced by ME, the N-terminally extended variant of *EVI1* containing an additional

PR-domain, *in vivo*.⁹ In synopsis of this recent report and our data, we suggest that EVI1 and ME share the property of p57 induction, although this has not been found in another experimental setting.⁹ Further experiments are required to explain the underlying variables. In line with our data, Konrad *et al.*¹⁵ saw a strong, dose-dependent cell cycle blockade mediated by human EVI1 in U937 cells, however without addressing the transcriptional response. The profound survival signal elicited by *Evi1* overexpression is also compatible with this previous report,¹⁵ which however, could not address the complex dynamics of proliferation and differentiation that we detected in our primary cell system.

Our data thus suggest a direct role of *Evi1* to confer resistance to proliferation and differentiation signals, and the magnitude of this effect might be dependent on the cytokine milieu. This may well contribute to the observed context dependence in the selection of EVI1 mutants observed in different gene therapy settings and non-human primate models.^{4,19,49–52}

Although we assessed the response to *Evi1* induction at an early time point (24 h), it remains to be determined which genes are direct transcriptional targets of this transcription factor. Altogether, our study establishes *Evi1* activation as an inducer of proliferative quiescence, but not as an inducer of completely irreversible senescence, coupled to a relative inhibition of differentiation. This function fits to its role in MDS as a slow disease, and in AML of poor prognosis, refractory to cytotoxic anti-proliferative drugs. Preleukemic dominance as a result of spontaneous chromosomal rearrangements or transgene integration events may thus be related to the better sleep of clones with induction of *Evi1*, rendering cells more refractory to the differentiation signals of stress hematopoiesis. Similar effects may be mediated by related genes such as *Prdm16*.^{5,53–55} Finally, our data suggest that for AML to develop after *Evi1* induction, selection for additional mutations must occur, possibly in pathways that are suppressed by *Evi1* activation or compensate its anti-proliferative effects.

We are aware of the limitation that our data were obtained in cultured murine hematopoietic progenitor cells. Of note, we and others found that prolonged *ex vivo* culture selects repopulating hematopoietic cells with insertional upregulation of *Evi1*,^{11,17–19} indicating that our findings are relevant in the context of genetic cell modification. Our inducible system may also be useful to study the immediate effect of *Evi1* overexpression on various hematopoietic subpopulations, including *bona fide* HSC. Additional *in vivo* experiments need to test the validity of the mechanisms and molecular targets suggested by the present study.

CONFLICT OF INTEREST

The authors declare no conflict of interest.

ACKNOWLEDGEMENTS

This work was supported by the German Research Foundation (DFG, Research priority program 1230 and cluster of excellence REBIRTH) and the European Union (grants Clinigene and CELL-PID). We thank Rena-Mareike Struss, Institute of Experimental Hematology, Hannover Medical School, Hannover, Germany, for help with breeding and genotyping of mice. We thank the Cell Sorting Unit of Hannover Medical School for support in sorting experiments. We are grateful to Marcel Tauscher, Institute of Cell and Molecular Pathology, Hannover Medical School, Hannover, Germany, for support in performing array-CGH analysis.

AUTHOR CONTRIBUTIONS

OSK, MS, A Schwarzer, A Schambach, TCH, MHB, NH, DS, MY and ZL performed experiments. SG and IR performed mathematical modeling. All authors analyzed data. CB and OSK designed the study, and wrote the manuscript. A Schwarzer, MHB, NH, ZL, SG, DS, BS contributed to writing the manuscript.

REFERENCES

- 1 Morishita K, Parker DS, Mucenski ML, Jenkins NA, Copeland NG, Ihle JN. Retroviral activation of a novel gene encoding a zinc finger protein in IL-3-dependent myeloid leukemia cell lines. *Cell* 1988; **54**: 831–840.
- 2 Li Z, Dullmann J, Schiedmeier B, Schmidt M, von Kalle C, Meyer J *et al.* Murine leukemia induced by retroviral gene marking. *Science* 2002; **296**: 497.
- 3 Kustikova O, Fehse B, Modlich U, Yang M, Dullmann J, Kamino K *et al.* Clonal dominance of hematopoietic stem cells triggered by retroviral gene marking. *Science* 2005; **308**: 1171–1174.
- 4 Calmels B, Ferguson C, Laukkanen MO, Adler R, Faulhaber M, Kim HJ *et al.* Recurrent retroviral vector integration at the Mds1/Evi1 locus in nonhuman primate hematopoietic cells. *Blood* 2005; **106**: 2530–2533.
- 5 Ott MG, Schmidt M, Schwarzwaelder K, Stein S, Siler U, Koehl U *et al.* Correction of X-linked chronic granulomatous disease by gene therapy, augmented by insertional activation of MDS1-EVI1, PRDM16 or SETBP1. *Nat Med* 2006; **12**: 401–409.
- 6 Lugthart S, Groschel S, Beverloo HB, Kayser S, Valk PJ, van Zelder-Bhola SL *et al.* Clinical, molecular, and prognostic significance of WHO type inv(3)(q21q26.2)/t(3;3)(q21;q26.2) and various other 3q abnormalities in acute myeloid leukemia. *J Clin Oncol* 2010; **28**: 3890–3898.
- 7 Groschel S, Lugthart S, Schlenk RF, Valk PJ, Eiwien K, Goudswaard C *et al.* High EVI1 expression predicts outcome in younger adult patients with acute myeloid leukemia and is associated with distinct cytogenetic abnormalities. *J Clin Oncol* 2010; **28**: 2101–2107.
- 8 Goyama S, Yamamoto G, Shimabe M, Sato T, Ichikawa M, Ogawa S *et al.* Evi-1 is a critical regulator for hematopoietic stem cells and transformed leukemic cells. *Cell Stem Cell* 2008; **3**: 207–220.
- 9 Zhang Y, Stehling-Sun S, Lezon-Geyda K, Juneja SC, Coillard L, Chatterjee G *et al.* PR-domain-containing Mds1-Evi1 is critical for long-term hematopoietic stem cell function. *Blood* 2011; **118**: 3853–3861.
- 10 Kataoka K, Sato T, Yoshimi A, Goyama S, Tsuruta T, Kobayashi H *et al.* Evi1 is essential for hematopoietic stem cell self-renewal, and its expression marks hematopoietic cells with long-term multilineage repopulating activity. *J Exp Med* 2011; **208**: 2403–2416.
- 11 Modlich U, Kustikova OS, Schmidt M, Rudolph C, Meyer J, Li Z *et al.* Leukemias following retroviral transfer of multidrug resistance 1 (MDR1) are driven by combinatorial insertional mutagenesis. *Blood* 2005; **105**: 4235–4246.
- 12 Maetzig T, Brugman MH, Bartels S, Heinz N, Kustikova OS, Modlich U *et al.* Polyclonal fluctuation of lentiviral vector-transduced and expanded murine hematopoietic stem cells. *Blood* 2011; **117**: 3053–3064.
- 13 Wolf S, Rudolph C, Morgan M, Busche G, Salguero G, Stripecke R *et al.* Selection for Evi1 activation in myelomonocytic leukemia induced by hyperactive signaling through wild-type NRas. *Oncogene*; e-pub ahead of print 30 July 2012; doi: 10.1038/onc.2012.329.
- 14 Haeflrich C, Bacher U, Haeflrich T, Dicker F, Alpermann T, Kern W *et al.* The inv(3)(q21q26)/t(3;3)(q21;q26) is frequently accompanied by alterations of the RUNX1, KRAS and NRAS and NF1 genes and mediates adverse prognosis both in MDS and in AML: a study in 39 cases of MDS or AML. *Leukemia* 2011; **25**: 874–877.
- 15 Konrad TA, Karger A, Hackl H, Schwarzinger I, Herbacek I, Wieser R. Inducible expression of EVI1 in human myeloid cells causes phenotypes consistent with its role in myelodysplastic syndromes. *J Leukoc Biol* 2009; **86**: 813–822.
- 16 Yoshimi A, Goyama S, Watanabe-Okochi N, Yoshiki Y, Nannya Y, Nitta E *et al.* Evi1 represses PTEN expression and activates PI3K/AKT/mTOR via interactions with polycomb proteins. *Blood* 2011; **117**: 3617–3628.
- 17 Du Y, Jenkins NA, Copeland NG. Insertional mutagenesis identifies genes that promote the immortalization of primary bone marrow progenitor cells. *Blood* 2005; **106**: 3932–3939.
- 18 Modlich U, Bohne J, Schmidt M, von Kalle C, Knoss S, Schambach A *et al.* Cell-culture assays reveal the importance of retroviral vector design for insertional genotoxicity. *Blood* 2006; **108**: 2545–2553.
- 19 Sellers S, Gomes TJ, Larochelle A, Lopez R, Adler R, Krouse A *et al.* *Ex vivo* expansion of retrovirally transduced primate CD34+ cells results in overrepresentation of clones with MDS1/EVI1 insertion sites in the myeloid lineage after transplantation. *Mol Ther* 2010; **18**: 1633–1639.
- 20 Magnusson M, Brun AC, Miyake N, Larsson J, Ehinger M, Bjornsson JM *et al.* HOXA10 is a critical regulator for hematopoietic stem cells and erythroid/megakaryocyte development. *Blood* 2007; **109**: 3687–3696.
- 21 Gossen M, Bujard H. Tight control of gene expression in mammalian cells by tetracycline-responsive promoters. *Proc Natl Acad Sci USA* 1992; **89**: 5547–5551.
- 22 Schambach A, Bohne J, Chandra S, Will E, Margison GP, Williams DA *et al.* Equal potency of gammaretroviral and lentiviral SIN vectors for expression of O6-methylguanine-DNA methyltransferase in hematopoietic cells. *Mol Ther* 2006; **13**: 391–400.
- 23 Li Z, Schwieger M, Lange C, Kraunus J, Sun H, van den Akker E *et al.* Predictable and efficient retroviral gene transfer into murine bone marrow repopulating cells using a defined vector dose. *Exp Hematol* 2003; **31**: 1206–1214.

- 24 Zhang CC, Lodish HF. Murine hematopoietic stem cells change their surface phenotype during *ex vivo* expansion. *Blood* 2005; **105**: 4314–4320.
- 25 Gentleman RC, Carey VJ, Bates DM, Bolstad B, Dettling M, Dudoit S et al. Bioconductor: open software development for computational biology and bioinformatics. *Genome Biol* 2004; **5**: R80.
- 26 Kauffmann A, Gentleman R, Huber W. arrayQualityMetrics—a bioconductor package for quality assessment of microarray data. *Bioinformatics* 2009; **25**: 415–416.
- 27 Gautier L, Cope L, Bolstad BM, Irizarry RA. affy—analysis of Affymetrix GeneChip data at the probe level. *Bioinformatics* 2004; **20**: 307–315.
- 28 Smyth G, Subramanian A, Tamayo P, Mootha VK, Mukherjee S, Ebert BL et al. Limma: linear models for microarray data. In: Gentleman R(ed) *Bioinformatics and Computational Biology Solutions Using R and Bioconductor*. Springer: New York, 2005, pp 397–420.
- 29 Subramanian A, Tamayo P, Mootha VK, Mukherjee S, Ebert BL, Gillette MA et al. Gene set enrichment analysis: a knowledge-based approach for interpreting genome-wide expression profiles. *Proc Natl Acad Sci USA* 2005; **102**: 15545–15550.
- 30 Culhane AC, Schwarzl T, Sultana R, Picard KC, Picard SC, Lu TH et al. GeneSigDB—a curated database of gene expression signatures. *Nucleic Acids Res* 2010; **38**: D716–D725.
- 31 Modlich U, Navarro S, Zychlinski D, Maetzig T, Knoess S, Brugman MH et al. Insertional transformation of hematopoietic cells by self-inactivating lentiviral and gammaretroviral vectors. *Mol Ther* 2009; **17**: 1919–1928.
- 32 Montini E, Cesana D, Schmidt M, Sanvito F, Bartholomae CC, Ranzani M et al. The genotoxic potential of retroviral vectors is strongly modulated by vector design and integration site selection in a mouse model of HSC gene therapy. *J Clin Invest* 2009; **119**: 964–975.
- 33 Forsberg EC, Prohaska SS, Katzman S, Heffner GC, Stuart JM, Weissman IL. Differential expression of novel potential regulators in hematopoietic stem cells. *PLoS Genet* 2005; **1**: e28.
- 34 Jaitin DA, Roisman LC, Jaks E, Gavutis M, Piehler J, Van der Heyden J et al. Inquiring into the differential action of interferons (IFNs): an IFN- α 2 mutant with enhanced affinity to IFNAR1 is functionally similar to IFN- β . *Mol Cell Biol* 2006; **26**: 1888–1897.
- 35 Kulaeva OI, Draghici S, Tang L, Kraniak JM, Land SJ, Tainsky MA. Epigenetic silencing of multiple interferon pathway genes after cellular immortalization. *Oncogene* 2003; **22**: 4118–4127.
- 36 Dauer DJ, Ferraro B, Song L, Yu B, Mora L, Buettner R et al. Stat3 regulates genes common to both wound healing and cancer. *Oncogene* 2005; **24**: 3397–3408.
- 37 Einav U, Tabach Y, Getz G, Yitzhaky A, Ozbek U, Amariglio N et al. Gene expression analysis reveals a strong signature of an interferon-induced pathway in childhood lymphoblastic leukemia as well as in breast and ovarian cancer. *Oncogene* 2005; **24**: 6367–6375.
- 38 Mathew R, Seiler MP, Scanlon ST, Mao AP, Constantinides MG, Bertozzi-Villa C et al. BTB-ZF factors recruit the E3 ligase cullin 3 to regulate lymphoid effector programs. *Nature* 2012; **491**: 618–621.
- 39 Rockova V, Abbas S, Wouters BJ, Erpelinck CA, Beverloo HB, Delwel R et al. Risk stratification of intermediate-risk acute myeloid leukemia: integrative analysis of a multitude of gene mutation and gene expression markers. *Blood* 2011; **118**: 1069–1076.
- 40 Li Q, Haigis KM, McDaniel A, Harding-Theobald E, Kogan SC, Akagi K et al. Hematopoiesis and leukemogenesis in mice expressing oncogenic NrasG12D from the endogenous locus. *Blood* 2011; **117**: 2022–2032.
- 41 Mirzayans R, Andrais B, Scott A, Murray D. New insights into p53 signaling and cancer cell response to DNA damage: implications for cancer therapy. *J Biomed Biotechnol*; e-pub ahead of print 15 July 2012; doi:10.1155/2012/170325.
- 42 Fridman AL, Tainsky MA. Critical pathways in cellular senescence and immortalization revealed by gene expression profiling. *Oncogene* 2008; **27**: 5975–5987.
- 43 Karakaya K, Herbst F, Ball C, Glimm H, Krämer A, Löffler H. Overexpression of EVI1 interferes with cytokinesis and leads to accumulation of cells with supernumerary centrosomes in G0/1 phase. *Cell Cycle* 2012; **11**: 3492–3503.
- 44 Stein S, Ott MG, Schultze-Strasser S, Jauch A, Burwinkel B, Kinner A et al. Genomic instability and myelodysplasia with monosomy 7 consequent to EVI1 activation after gene therapy for chronic granulomatous disease. *Nat Med* 2010; **16**: 198–204.
- 45 Kohlmann AL, Bullinger C, Thiede M, Schaich S, Schnittger KD, Döhner K et al. Gene expression profiling in AML with normal karyotype can predict mutations for molecular markers and allows novel insights into perturbed biological pathways. *Leukemia* 2010; **24**: 1216–1220.
- 46 Alimonti A, Nardella C, Chen Z, Clohessy JG, Carracedo A, Trotman LC et al. A novel type of cellular senescence that can be enhanced in mouse models and human tumor xenografts to suppress prostate tumorigenesis. *J Clin Invest* 2010; **120**: 681–693.
- 47 Kustikova OS, Geiger H, Li Z, Brugman MH, Chambers SM, Shaw CA et al. Retroviral vector insertion sites associated with dominant hematopoietic clones mark 'stemness' pathways. *Blood* 2007; **109**: 1897–1907.
- 48 Matsumoto A, Takeishi S, Kanie T, Susaki E, Onoyama I, Tateishi Y et al. p57 is required for quiescence and maintenance of adult hematopoietic stem cells. *Cell Stem Cell* 2011; **9**: 262–271.
- 49 Aiuti A, Cattaneo F, Galimberti S, Benninghoff U, Cassani B, Callegaro L et al. Gene therapy for immunodeficiency due to adenosine deaminase deficiency. *N Engl J Med* 2009; **360**: 447–458.
- 50 Gaspar HB, Björkregren E, Parsley K, Gilmour KC, King D, Sinclair J et al. Successful reconstitution of immunity in ADA-SCID by stem cell gene therapy following cessation of PEG-ADA and use of mild preconditioning. *Mol Ther* 2006; **14**: 505–513.
- 51 Hacein-Bey-Abina S, Garrigue A, Wang GP, Soulier J, Lim A, Morillon E et al. Insertional oncogenesis in 4 patients after retrovirus-mediated gene therapy of SCID-X1. *J Clin Invest* 2008; **118**: 3132–3142.
- 52 Boztug K, Schmidt M, Schwarzer A, Banerjee PP, Diez IA, Dewey RA et al. Stem-cell gene therapy for the Wiskott-Aldrich syndrome. *N Engl J Med* 2010; **363**: 1918–1927.
- 53 Aguilo F, Avagyan S, Labar AS, Sevilla A, Lee DF, Kumar P et al. Prdm16 is a physiological regulator of hematopoietic stem cells. *Blood* 2011; **117**: 5057–5066.
- 54 Chuikov S, Levi BP, Smith ML, Morrison SJ. Prdm16 promotes stem cell maintenance in multiple tissues, partly by regulating oxidative stress. *Nat Cell Biol* 2010; **12**: 999–1006.
- 55 Modlich U, Schambach A, Brugman MH, Wicke DC, Knoess S, Li Z et al. Leukemia induction after a single retroviral vector insertion in *Evi1* or *Prdm16*. *Leukemia* 2008; **22**: 1519–1528.
- 56 Tesio M, Trumpp A. Breaking the cell cycle of HSCs by p57 and friends. *Cell Stem Cell* 2011; **9**: 187–192.

Supplementary Information accompanies the paper on the Leukemia website (<http://www.nature.com/leu>)